Tumors mimic the niche to inhibit neighboring stem cell differentiation

Yang Zhang[1], Yuejia Wang[1], Jinqiao Song[1], Lizhong Yan[1], Ziguang Wang[1], Dongze Song[1], Yudi Zhao[1], and Shaowei Zhao[1,2]*

[1]Department of Genetics and Cell Biology, College of Life Sciences, Nankai University, Tianjin, 300071, People's Republic of China

[2]Lead contact

* For correspondence: swzhao@nankai.edu.cn

Abstract

Although it is well-established that stem cells maintain tissue homeostasis while tumors disrupt it, the mechanisms by which tumors influence the development of nearby stem cells remain poorly understood. Using *Drosophila* ovaries as a model system, here we discovered that *bam* or *bgcn* mutant germline tumors inhibit the differentiation of neighboring wild-type germline stem cells (GSCs). Mechanistically, these tumor cells mimic the stem cell niche by secreting the BMP ligands Dpp and Gbb, but at reduced levels, resulting in moderate BMP signaling activation in adjacent GSCs. Such BMP signaling activation is sufficient to repress *bam* transcription, thereby blocking GSC differentiation. To our knowledge, this is the first example that tumors can functionally mimic a stem cell niche to inhibit the differentiation of neighboring wild-type stem cells. Similar regulatory paradigms may operate in mammalian tissues, including humans, during tumorigenesis.

Key words: *bam*, BMP signaling, tumors, germline stem cell, stem cell niche, *Drosophila*

Introduction

The homeostasis of many tissues in our bodies is maintained by adult stem cells, but this balance can be disrupted by tumor cells. What occurs when tumorigenesis intersects with stem cell development? To address this question, a mosaic-analysis model system is essential, where wild-type stem cells develop alongside tumor cells. *Drosophila* offers an exceptional model for such studies, as it allows for the efficient generation of mosaic clones through various established methods *(**Germani et al., 2018; Pastor-Pareja and Xu, 2013**)*.

In *Drosophila* ovaries, germline stem cells (GSCs) play a crucial role in sustaining normal oogenesis and maintaining fertility *(**Fuller and Spradling, 2007; Lin, 1997**)*. These GSCs reside in a specialized microenvironment known as the stem cell niche (hereafter referred to as niche) *(**Xie and Spradling, 2000**)*. Typically, a GSC undergoes asymmetric division, generating two distinct daughter cells: one remains in the niche to self-renew as a GSC, while the other, called a cystoblast, exits the niche and initiates differentiation. During the differentiation process, each cystoblast performs exactly four rounds of mitotic division with incomplete cytokinesis to produce16 interconnected cystocytes, forming a germline cyst. In each germline cyst, only one germ cell is destined to become the oocyte, while the remaining 15 differentiate into nurse cells that support the development of the oocyte (***Figure 1A***) *(**Fuller and Spradling, 2007; Lin, 1997**)*. The principal niche signals are bone morphogenetic protein (BMP) ligands, including Decapentaplegic (Dpp) and Glass bottom boat (Gbb), which are secreted predominantly by cap cells, the major somatic niche cells (Chen and McKearin, 2003a; Li et al., 2016; Song et al., 2004; Xie and Spradling, 1998, 2000). These ligands activate BMP signaling in GSCs, leading to the transcriptional repression of *bag of marbles* (*bam*), a key gene that promotes differentiation. In contrast, BMP signaling is inactive in cystoblasts, allowing Bam to be expressed and drive their

49 differentiation (***Chen and McKearin, 2003a; Song et al., 2004***). Bam carries out this
50 function in collaboration with its partner, Benign gonial cell neoplasm (Bgcn) (***Li et al.,***
51 ***2009; Ohlstein et al., 2000***).

52 GSCs mutant for *bam* or *bgcn* fail to differentiate and instead hyper-proliferate,
53 forming a well-established *Drosophila* germline tumor model (***Lavoie et al., 1999;***
54 ***McKearin and Ohlstein, 1995; McKearin and Spradling, 1990; Niki and Mahowald,***
55 ***2003***). Notably, these germline tumor cells competitively displace wild-type GSCs from
56 the niche (***Jin et al., 2008***). The resulting displacement creates a microenvironment
57 where wild-type GSCs are surrounded by tumor cells, providing an excellent model
58 system to study stem cell behavior in tumor neighborhoods.

59 Here, we demonstrate that *bam* or *bgcn* mutant germline tumors inhibit the
60 differentiation of neighboring wild-type GSCs by functionally mimicking the stem cell
61 niche. This mechanism may be conserved in mammals, including humans, during
62 tumorigenesis, where malignant cells could similarly disrupt normal stem cell
63 development.

Results

Germline tumors inhibit the differentiation of neighboring wild-type GSCs

Using the *nos>FLP/FRT* or *hs-FLP/FRT* methods we previously established (***Zhang et al., 2023; Zhao et al., 2018***), we generated *bam* or *bgcn* mutant germline clones in *Drosophila* ovaries (***Figure 1B***). Surprisingly, we found that many wild-type germ cells located outside the niche retained a GSC-like single-germ-cell (SGC) morphology, even when encapsulated within egg chambers (***Figure 1C, D, Figure 1—figure supplement 1***). Under normal conditions, GSCs that exit the niche differentiate into interconnected germline cysts, where germ cells are linked rather than remaining as individual, isolated cells (***Fuller and Spradling, 2007; Xie and Spradling, 2000***). To rule out the possibility that the SGC phenotype is an artifact caused by GFP expression, we repeated the experiments using RFP and arm-lacZ as alternative mosaic-analysis markers. Consistent results were observed (***Figure 1E, F***), confirming that the phenotype is not attributable to GFP.

To further confirm that these SGCs exhibit GSC-like characteristics, we conducted anti-α-Spectrin immunofluorescent staining, a method that labels a germline-specific organelle known as the spectrosome in GSCs and cystoblasts, and the fusome in cystocytes. GSCs perform complete cell division, whereas cystocytes undergo incomplete cytokinesis, remaining interconnected through fusomes and ring canals. Consequently, spectrosomes appear as dot-like structures, while fusomes exhibit branched morphologies (***Figure 1G***) (***Lin et al., 1994***). To accurately capture the three-dimensional (3D) architecture of spectrosomes and fusomes, we acquired z-stack images using confocal microscopy. Strikingly, these SGCs displayed dot-like spectrosomes, closely resembling those observed in wild-type GSCs and *bam* or *bgcn* mutant GSC-like tumor cells (***Figure 1H, I***). We also considered the possibility that SGCs might arise through the dedifferentiation of the cystocytes in germline cysts

90 surrounded by germline tumors. If this were the case, such cystocytes would initially
91 undergo complete cell division, leaving behind midbodies as markers of the late
92 cytokinesis stage. When visualized by anti-α-Spectrin immunofluorescence, midbody
93 appears as a central sphere that is slightly connected to two larger flanking structures,
94 resembling a variant of nunchucks (***Mathieu et al., 2022***). Notably, in our analyses of
95 over 50 germline cysts surrounded by *bam* mutant germline tumors, none contained
96 midbodies, suggesting that dedifferentiation is unlikely to be the primary mechanism
97 responsible for the SGC phenotype. Together, these findings indicate that *bam* or *bgcn*
98 mutant germline tumors inhibit the differentiation of neighboring wild-type GSCs.

99 **The inhibition of differentiation in SGCs relies on the lack of Bam expression**

100 Given that Bam is the key factor promoting GSC differentiation (***McKearin and***
101 ***Ohlstein, 1995; Ohlstein and McKearin, 1997***), we were very curious about the
102 expression of Bam in SGCs. At first, we assessed Bam protein levels using
103 immunofluorescent staining with an anti-BamC antibody (***McKearin and Ohlstein,***
104 ***1995***). Strikingly, none of the SGCs examined (n > 100) were BamC-positive (***Figure***
105 ***2A***). Then, we analyzed *bam* transcription levels using a *bamP*-GFP reporter (***Chen and***
106 ***McKearin, 2003b***). Under normal conditions, 100% of GSCs within the niche (n = 153)
107 were GFP-negative, while 98% of cystoblasts (n = 106) were GFP-positive (***Figure 2B,***
108 ***C***), confirming that *bam* transcription is associated with the initiation of GSC
109 differentiation (***McKearin and Ohlstein, 1995***). Notably, 74% of SGCs (n = 132) were
110 GFP-negative, while the remaining 26% were GFP-positive (***Figure 2B, C***). This
111 suggests that SGCs can be categorized into two distinct groups: those resembling GSCs
112 (GSC-like) and those resembling cystoblasts (cystoblast-like). The cystoblast-like SGCs
113 may have already initiated their differentiation program toward becoming cystocytes.
114 Since *bam* transcription initiates in cystoblasts (***McKearin and Spradling, 1990***) but
115 Bam proteins accumulate predominantly in cystocytes (***McKearin and Ohlstein, 1995***),

116 the Bam protein levels in these cystoblast-like SGCs are likely below the detection
117 threshold at this early stage.

118 Next, we asked whether ectopic expression of Bam can drive SGCs to
119 differentiate. To address this, we established two experimental scenarios: one with the
120 *hs-bam* element and one without as the control. In the *hs-bam* scenario (*with hs-bam*),
121 GFP-positive germ cells are wild-type (carrying *hs-bam*), while GFP-negative cells are
122 *bam*$^{-/-}$ (lacking *hs-bam*). In the control scenario (*without hs-bam*), GFP-positive cells are
123 wild-type, and GFP-negative cells are *bam*$^{-/-}$ (***Figure 2D***, see genotypes in ***Source data***
124 ***1***). To quantify the SGC phenotype, we calculated the percentage of SGCs relative to the
125 total number of SGCs and germline cysts, considering the out-of-niche germ cells that
126 are either fully enclosed by germline tumors (e.g., the right SGC in ***Figure 1I*** and the
127 marked germline cyst in ***Figure 2G***) or in contact with wild-type germ cells or somatic
128 cells on just one side (e.g., the left SGC in ***Figure 1I*** and the outlined germline cyst in
129 ***Figure 4C***). Although the SGC phenotype was detectable after fly eclosion, we
130 quantified it in 14-day-old flies to ensure robust germline tumor growth, improving
131 quantification efficiency. To induce ectopic Bam expression, 12-day-old female flies were
132 subjected to heatshock treatment, which involved heating at 37°C for two hours, twice
133 daily with a 6-hour interval, and over two consecutive days. In the absence of heatshock
134 treatment, the percentage of SGCs in ovaries of both genotypes showed no significant
135 difference at either 12 or 14 days (***Figure 2E-H***), indicating that the *hs-bam* element
136 alone, without heatshock, does not affect the phenotype. However, following heatshock
137 treatment, the percentage of SGCs in ovaries with *hs-bam* was markedly reduced
138 compared to those without *hs-bam* (***Figure 2E-H***), suggesting that ectopic Bam
139 expression can drive SGCs to differentiate. Collectively, these results support that the
140 differentiation defects of SGCs are due to the lack of Bam expression.

141 **SGCs retain moderate BMP signaling activation**

142 Within the niche, BMP signaling functions to repress *bam* transcription to inhibit GSC
143 differentiation (***Chen and McKearin, 2003a; Song et al., 2004***). To investigate BMP
144 signaling activation in SGCs, we employed immunofluorescent staining for pMad, a well-
145 characterized marker of BMP signaling activity (***Kai and Spradling, 2003***). Surprisingly,
146 we observed undetectable pMad levels in all SGCs examined (n > 100) (***Figure 3A, B***).
147 To investigate this further, we examined the activity of *Dad*-lacZ, a highly sensitive BMP
148 signaling reporter known to be activated not only in GSCs but also in cystoblasts (***Kai***
149 ***and Spradling, 2003; Song et al., 2004***). Notably, 73% of SGCs were lacZ-positive (n =
150 107), a proportion lower than that of GSCs within the niche, which showed 100% lacZ
151 positivity (n = 122) (***Figure 3C, D***). Furthermore, when comparing *Dad*-lacZ expression
152 levels exclusively in lacZ-positive cells, we found that SGCs exhibited significantly lower
153 expression levels than GSCs within the niche (***Figure 3C, E***). These findings indicate
154 that BMP signaling is activated in SGCs but at lower levels than those in GSCs within
155 the niche.

156 Beyond maintaining *Drosophila* female GSCs in the niche, BMP signaling also
157 promotes their division (***Xie and Spradling, 1998***). Since the activation levels of BMP
158 signaling in SGCs were lower than those in GSCs within the niche, we hypothesized that
159 SGCs would exhibit slower proliferation rates than GSCs. To test this hypothesis, we
160 performed BrdU incorporation assays. The results revealed that only 4.5% of SGCs
161 were BrdU-positive (n = 1034), a significantly lower proportion than the 7.8% observed in
162 GSCs within the niche (n = 1337) (***Figure 3F-H***). These findings further corroborate the
163 reduced activation of BMP signaling in SGCs relative to GSCs.

164 **BMP signaling inhibits SGC differentiation**

165 Then we investigated whether BMP signaling functions to inhibit SGC differentiation. The
166 BMP type II receptor Punt and the co-Smad Medea (Med) are essential for maintaining
167 GSC stemness within the niche (***Xie and Spradling, 1998***). To investigate whether they

168 are also required to inhibit SGC differentiation, we established a genetic scenario, in
169 which GFP$^{+/+}$ RFP$^{-/-}$ germ cells are *punt*$^{-/-}$ or *med*$^{-/-}$; GFP$^{+/-}$ RFP$^{+/-}$ germ cells are *punt*$^{+/-}$
170 *bam*$^{+/-}$ or *med*$^{+/-}$ *bam*$^{+/-}$ (similar to wild-type); and GFP$^{-/-}$ RFP$^{+/+}$ germ cells are *bam*$^{-/-}$. In
171 control experiments (with no *punt* or *med* mutation), GFP$^{+/+}$ RFP$^{-/-}$ germ cells are wild-
172 type; GFP$^{+/-}$ RFP$^{+/-}$ germ cells are *bam*$^{+/-}$ (similar to wild-type); and GFP$^{-/-}$ RFP$^{+/+}$ germ
173 cells are *bam*$^{-/-}$ (***Figure 4A***, see genotypes in ***Source data 1***). Strikingly, the proportion
174 of *punt*$^{-/-}$ or *med*$^{-/-}$ SGCs relative to total SGCs was significantly lower than in controls
175 (***Figure 4B-E***). Conversely, among *punt*$^{-/-}$ or *med*$^{-/-}$ germ cells meeting our established
176 criteria for SGC phenotype quantification, germline cysts constituted a higher percentage
177 compared to controls (***Figure 4F***). These results indicate that Punt and Med function to
178 inhibit SGC differentiation.

179 Mothers against dpp (Mad) is the primary transcription factor of BMP signaling,
180 and it is also essential for GSC maintenance in *Drosophila* ovaries (***Xie and Spradling,***
181 ***1998***). Unlike *punt* and *med*, which reside on the same chromosome arm (3R) as *bam*,
182 *mad* is located on a separate chromosome arm (2L). To investigate whether Mad is
183 required to inhibit SGC differentiation, we established a genetic scenario, in which GFP$^{-/-}$
184 germ cells are *mad*$^{-/-}$ and GFP$^{+/+}$ germ cells are *bam*$^{-/-}$. In control experiments (with no
185 *mad* mutation), GFP$^{-/-}$ germ cells are wild-type and GFP$^{+/+}$ germ cells are *bam*$^{-/-}$ (***Figure***
186 ***4G***, see genotypes in ***Source data 1***). Notably, *mad* mutation significantly decreased the
187 SGC proportion relative to controls (***Figure 4H-J***). These results suggest that, like Punt
188 and Med, Mad also plays a crucial role in suppressing SGC differentiation. Together,
189 these findings demonstrate that BMP signaling contributes to inhibiting SGC
190 differentiation, despite at reduced activation levels.

191 **Germline tumors secret Dpp and Gbb**

192 The next question we sought to address was which cells surrounding SGCs secrete
193 BMP ligands, such as Dpp and Gbb. Guided by the Occam's Razor principle, we

194 focused on *bam* or *bgcn* mutant germline tumor cells, as the SGC phenotype is
195 dependent on their presence. Initial attempts to detect expression of these two ligand
196 genes using *in situ* hybridization proved unsuccessful. We therefore employed an
197 established *dpp*-lacZ (*P4*-lacZ) reporter (***Li et al., 2016***) to monitor Dpp expression.
198 Consistent with previous findings, we observed robust lacZ signals in cap cells (***Figure***
199 ***5A***), the primary niche cells that are responsible for BMP ligand secretion (***Chen and***
200 ***McKearin, 2003a; Song et al., 2004; Xie and Spradling, 2000***). Notably, *bam* mutant
201 germline tumor cells displayed lower lacZ expression levels than cap cells but
202 significantly higher levels than differentiating cystocytes (***Figure 5A-C***).

203 To more sensitively assess Dpp and Gbb expression, we performed real-time
204 quantitative PCR (RT-qPCR) analyses in *bam* or *bgcn* mutant ovaries, comparing
205 samples with and without germline-specific knockdown of *dpp* or *gbb*. Detection of
206 reduced transcript levels in knockdown conditions would confirm active expression of
207 these genes in the respective genetic backgrounds. Consistent with the essential roles
208 of these two genes in fly viability, ubiquitous knockdown using *act-GAL4* with either *dpp-*
209 *RNAi* or *gbb-RNAi* caused lethality, which results also validated the efficacy of these
210 RNAi lines. Notably, germline-specific knockdown of *dpp* or *gbb* significantly reduced
211 their transcript levels compared to *yellow* (*y*) or *white* (*w*) knockdown controls (***Figure***
212 ***5D, E***). These findings demonstrate that *bam* or *bgcn* mutant germline tumors secrete
213 the BMP ligands, albeit at lower levels than cap cells.

214 **Dpp and Gbb secreted by germline tumors are required to inhibit SGC**
215 **differentiation**

216 Finally, we investigated whether Dpp and Gbb secreted by germline tumors are required
217 to inhibit SGC differentiation. Using a previously established double-mutant mosaic-
218 analysis strategy for two genes on different chromosomes (***Zhang et al., 2024; Zhang***
219 ***et al., 2023***), we generated *dpp bam* or *gbb bam* double-mutant germline clones using

220 two *dpp* mutant alleles, dpp^{d6}, dpp^{d12}, and one *gbb* allele, gbb^{1} (***Figure 6A, B***, see
221 genotypes in ***Source data 1***). Heterozygotes in any of these alleles did not affect GSC
222 maintenance, germ cell differentiation, and female fly fertility (***Figure 6—figure***
223 ***supplement 1***). However, both *dpp bam* and *gbb bam* double-mutant germline tumor
224 cells exhibited reduced proliferation rates compared to *bam* single-mutant controls
225 (***Figure 6—figure supplement 2***), indicating that autocrine BMP signaling promotes
226 *bam* mutant tumor growth. As mentioned earlier, our evaluation focused on germ cells
227 that have exited the niche and are surrounded by germline tumors to quantify the SGC
228 phenotype. However, this raises the question of whether the extent of tumor
229 encirclement (i.e., being surrounded by more or fewer tumor cells) influences the
230 phenotype. To investigate this, we compared the SGC phenotype in bigger and smaller
231 *bam* mutant germline tumors. Using confocal microscopy, we analyzed 70 germaria
232 containing *bam* mutant germline clones that met our criteria for SGC phenotype
233 quantification. For each *bam* mutant germline clone, we scanned and measured its
234 maximal 2D cross-sectional area as a proxy for its 3D size. The 35 bigger and 35
235 smaller clones were categorized as 'bigger' and 'smaller' tumors, respectively. Strikingly,
236 we observed no significant difference in the SGC phenotype between these two groups
237 of tumors (***Figure 6—figure supplement 3***), suggesting that direct contact between
238 tumorous and wild-type germ cells, rather than tumor size, is the primary determinant of
239 this phenotype.

240 The results above demonstrate that comparing the severity of the SGC
241 phenotype is feasible between germ cells surrounded by smaller *dpp bam* or *gbb bam*
242 double-mutant germline tumors and those surrounded by larger *bam* single-mutant
243 germline tumors. Remarkably, both *dpp bam* and *gbb bam* double-mutant germline
244 tumors enclosed fewer SGCs but more germline cysts than their *bam* single-mutant
245 counterparts (***Figure 6C-I***). Thus, we concluded that the BMP ligands from directly-

246 contacting germline tumor cells mediate the dominant inhibition of SGC differentiation.
247 This amazingly parallels the mechanism observed in normal stem cell niche, where only
248 germ cells in direct contact with cap cells are maintained as GSCs (***Chen and***
249 ***McKearin, 2003a; Song et al., 2004; Xie and Spradling, 2000***).

250 **Discussion**

251 Our study reveals that *bam* or *bgcn* mutant germline tumors in *Drosophila* ovaries
252 secrete lower levels of BMP ligands Dpp and Gbb than cap cells, resulting in moderate
253 BMP signaling activation in adjacent wild-type GSCs (called SGCs in this study). Such
254 BMP signaling activation is sufficient to repress *bam* transcription, thereby blocking SGC
255 differentiation (see our working model in ***Figure 7***). Strikingly, this mechanism closely
256 recapitulates the normal niche signaling program mediated by cap cells (***Chen and***
257 ***McKearin, 2003a; Song et al., 2004; Xie and Spradling, 1998, 2000***). To our
258 knowledge, this represents the first evidence that tumor cells can functionally mimic a
259 stem cell niche to arrest neighboring wild-type stem cells in an undifferentiated state.

260 *bam* or *bgcn* mutant germline tumors consist of GSC-like cells (***Lavoie et al.,***
261 ***1999; McKearin and Ohlstein, 1995***), which are expected to resemble SGCs. However,
262 out-of-niche *bgcn* mutant germline tumor cells did not activate BMP signaling to the
263 same extent as SGCs, as evidenced by much lower *Dad*-lacZ expression in GFP-
264 negative *bgcn* mutant tumor cells than in neighboring GFP-positive SGCs (***Figure 3C***).
265 Consistent with this, while only 26% of SGCs expressed *bamP*-GFP, most of out-of-
266 niche *bam* mutant germline tumor cells were *bamP*-GFP-positive (***Figure 2B, C***), further
267 supporting reduced BMP signaling in these tumor cells relative to SGCs. These findings
268 suggest that SGCs are more responsive to BMP signals secreted by germline tumors
269 than the tumors themselves. Future studies are needed to elucidate the underlying
270 mechanisms.

271 One interesting finding is that *bam* or *bgcn* mutant germline tumors secrete lower
272 levels of BMP ligands than cap cells (***Figure 5A-C***). This aligns with earlier microarray
273 data showing that purified *Drosophila* female GSCs express minimal Dpp and Gbb (***Kai***
274 ***et al., 2005***). However, our work reveals that such BMP levels in germline tumors are
275 functionally critical to suppress SGC differentiation (***Figure 6***). Unlike normal GSCs,

276 which receive unidirectional BMP ligands from cap cells (***Chen and McKearin, 2003a;***
277 ***Li et al., 2016; Song et al., 2004; Xie and Spradling, 2000***), SGCs are often fully
278 surrounded by *bam* or *bgcn* mutant germline tumors. This spatial advantage likely
279 enables tumors to inhibit SGC differentiation efficiently without matching the high BMP
280 output of cap cells. Moreover, since BMP signaling is known to both inhibit normal GSC
281 differentiation and promote their proliferation (***Xie and Spradling, 1998***), it should
282 similarly stimulate SGC expansion, which is detrimental for *bam* or *bgcn* mutant germline
283 tumors. We propose that these tumor cells finely regulate BMP secretion to balance
284 these opposing demands: maintaining differentiation blockade of SGCs while avoiding
285 stimulation of their excessive proliferation.

286 A well-established principle in oncology is that tumor aggressiveness correlates
287 with poor differentiation, with less-differentiated tumors exhibiting enhanced
288 transformative capacity and metastatic potential (***Jogi et al., 2012; Lytle et al., 2018***). In
289 *Drosophila* ovaries, *bam* or *bgcn* mutant germline tumors consist of GSC-like cells that
290 may resemble these poorly differentiated human tumors (***Lavoie et al., 1999; McKearin***
291 ***and Ohlstein, 1995***). This similarity raises the possibility that stem cell-like human
292 tumors may similarly inhibit the differentiation of adjacent wild-type stem cells. By
293 blocking differentiation, such tumors could deplete terminally differentiated cell
294 populations, potentially exacerbating patient mortality. This mechanism may contribute to
295 the heightened lethality of poorly differentiated tumors. Further investigation is needed to
296 test this hypothesis.

297 The differentiation of a single GSC into a 16-cell germline cyst, comprising 15
298 polyploid nurse cells and one developing oocyte, represents a substantial metabolic
299 investment (***Fuller and Spradling, 2007; Lin, 1997***). We propose that *bam* or *bgcn*
300 mutant germline tumors block this process to divert nutrients toward their own
301 uncontrolled growth. This phenomenon could have broad implications, as many human

tissues and organs (intestine, muscle, skin, blood system, male germline, etc.) similarly depend on adult stem cells for homeostasis (***Blanpain and Fuchs, 2006; Gehart and Clevers, 2019; Sousa-Victor et al., 2022; Spradling et al., 2011; Wilkinson et al., 2020***). Notably, these stem cell-dependent tissues and organs are frequent sites of tumorigenesis, raising the possibility that human cancers may similarly impair neighboring stem cell differentiation to optimize nutrient allocation for malignant growth. A key limitation of our study is that the evidence is derived solely from *Drosophila* germline. Future work should explore whether similar regulatory paradigms operate in mammalian tissues during tumorigenesis.

311 **Materials and Methods**

312 **Key resources table**

Reagent or Resource	Source	Identifier
Antibodies		
mouse anti-α-Spectrin	Developmental Studies Hybridoma Bank, DSHB	3A9
mouse anti-BamC	DSHB	AB_10570327
mouse anti-β-Gal	DSHB	JIE7
mouse anti-BrdU	Sigma	B5002
rabbit anti-pMad	Ed Laufer	N/A
rabbit anti-Vasa	Zhaohui Wang	(***Chen et al., 2014***)
goat anti-mouse 546	Invitrogen	A11003
goat anti-rabbit 488	Apexbio	K1206
goat anti-rabbit 546	Invitrogen	A11035
cDNA clone		
bam cDNA clone	Berkeley *Drosophila* Genome Project, BDGP	FI05606
***Drosophila* strains**		
act-GAL4	Zhaohui Wang	N/A
bam^{BG} (strong loss-of-function allele)	Zhaohui Wang	(***Chen and McKearin, 2005***)
$bam^{\Delta 86}$ (null allele)	Michael Buszczak	(***Bopp et al., 1993***)

bamP-GFP	Ting Xie	(***Chen and McKearin, 2003b***)
bgcn^{1} (null allele)	Bloomington *Drosophila* Stock Center, BDSC	6054
Canton-S	BDSC	64349
Dad-lacZ	Zheng Guo	(***Kai and Spradling, 2003***)
dpp^{d6} (hypomorphic allele)	BDSC	2062
dpp^{d12} (hypomorphic allele)	BDSC	2070
dpp(P4)-lacZ	Rongwen Xi	(***Li et al., 2016***)
EGFP FRT40A	BDSC	5629
FRT40A	BDSC	1816
FRT42D	BDSC	1802
FRT42D EGFP	BDSC	5626
FRT82B	BDSC	86313
FRT82B arm-lacZ	BDSC	7369
FRT82B EGFP	BDSC	32655
FRT82B RFP	BDSC	30555
gbb^{1} (null allele)	BDSC	98344
hs-bam on chromosome 3R	this study	N/A
mad^{12} (null allele)	BDSC	51301
med^{1} (null allele)	BDSC	9033
nos-GAL4-VP16	Ruth Lehmann	(***Van Doren et al., 1998***)
P{bam+}	Shaowei Zhao	(***Zhang et al., 2023***)
punt^{135} (strong loss-of-function allele)	BDSC	3100

UASp-dpp-RNAi-1	TsingHua Fly Center, THFC	TH201500984.S
UASp-dpp-RNAi-2	THFC	THU5880
UASp-FLP	Shaowei Zhao	(***Zhang et al., 2023***)
UASp-gbb-RNAi	THFC	THU1480
UASp-GFP	Michael Buszczak	N/A
UASp-yellow-RNAi	THFC	TH03150.N
UASz-FLP	Shaowei Zhao	(***Zhang et al., 2023***)
Kits		
ChamQ SYBR qPCR Master Mix	Vazyme	Q311
HiFiScript cDNA Synthesis Kit	CWBIO	CW2569M
RNeasy Micro Kit	Qiagen	74004
Plasmids		
bam cDNA clone	Berkeley *Drosophila* Genome Project	FI05606
pCaSpeR-hs	Eric Baehrecke	N/A
attB-pCaSpeR-hs-bam	this study	N/A
Software		
Adobe Photoshop 2022	San Jose, CA, USA	
ImageJ	NIH	
Prism	Graphpad Software, Inc.	
ZEN 3.0 SR imaging software	Carl Zeiss	

313

314 **Data availability**

315 All genotypes are described in **Source data 1**, and the raw quantification data are
316 included in **Source data 2**.

317 **Fly husbandry**

318 Flies were raised at 25°C on standard cornmeal/molasses/agar media.

319 **Transgenic flies**

320 ***hs-bam* on chromosome 3R**: The coding sequence of the *bam* gene, amplified from
321 the cDNA clone, was cloned into the *BglII-XbaI* sites of the *pCaSpeR-hs* vector (a gift
322 from Eric Baehrecke), while the *attB* sequence was inserted into the *XhoI* site. The
323 resulting *attB-pCaSpeR-hs-bam* plasmid was then microinjected into the *attP154*
324 (Chromosome 3R*, 97D2*) fly strain to generate site-specific transgenic flies.

325 **Heatshock method to induce germline clones**

326 To ensure developmental synchrony and maintain low-density growth, eggs within 8
327 hours of laying were collected for heatshock treatment. The animals (late-Larva 3/early-
328 Pupa stage) were subjected to twice-daily heatshocks at 37°C (2 hours per session, with
329 a 6-hour interval between the two sessions) for 6 consecutive days.

330 **Fertility test**

331 For each genotype, three independent crosses were performed. Each cross vial
332 contained two females and four w^{1118} (wild-type) males, all aged three days old. The
333 crosses were transferred to fresh vials every two days, with five replicate vials quantified
334 per genotype. After all adult flies eclosed, offspring production was assessed by counting
335 the number of empty pupae on the vial walls.

336 **BrdU labeling**

337 Ovaries were dissected in Schneider's insect medium (SIM) and incubated in freshly
338 prepared BrdU solution (100 μg/mL in SIM) for five hours at 25°C. After washing with
339 PBS (30 min), samples were fixed in 4% paraformaldehyde (PBS-diluted) for three
340 hours, followed by another PBS wash (30 min). Samples were then treated with RQ1

341 DNase reaction solution (Promega, Madison, WI, USA) for one hour, washed with PBST
342 (0.3% Triton X-100 in PBS, 30 min), and incubated overnight at 4°C with mouse anti-
343 BrdU antibody. Following a PBST wash (one hour), ovaries were incubated with goat
344 anti-mouse 546 and DAPI (0.1 μg/mL) in PBST for three hours, washed again in PBST
345 (one hour), and mounted in 70% glycerol (autoclaved).

346 **Immuno-florescent staining, image collection, and data Processing**

347 Ovaries were dissected in PBS, fixed in 4% paraformaldehyde (in PBS) for three hours,
348 washed with PBST (0.3% Triton X-100 in PBS) for 30 min, and then incubated overnight
349 at 4°C with primary antibodies diluted in PBST as follows: mouse anti-BamC (1:5),
350 mouse anti-β-Gal (1:200), mouse anti-α-Spectrin (1:100), rabbit anti-pMad (1:500), and
351 rabbit anti-Vasa (1:2000). After washing with PBST (one hour), samples were incubated
352 with Alexa Fluor-conjugated secondary antibodies (1:1000) and 0.1 μg/mL DAPI (in
353 PBST) for three hours, followed by a final PBST wash (one hour). Ovaries were mounted
354 in 70% glycerol and imaged using a Zeiss LSM 710 confocal microscope (Carl Zeiss AG,
355 Baden-Württemberg, Germany). Images were processed with ZEN 3.0 SR imaging
356 software (Carl Zeiss) and Adobe Photoshop 2022. The quantification data were
357 processed by Microsoft Excel or GraphPad Prism.

358 **RT-qPCR**

359 Ovaries from 14-day-old flies were dissected, and total RNA was extracted using the
360 RNeasy Micro Kit. Equal amounts of RNA were reverse-transcribed into cDNA using the
361 HiFiScript cDNA Synthesis Kit. RT-qPCR was performed on a CFX Connect Real-Time
362 PCR System (Bio-Rad) with ChamQ SYBR qPCR Master Mix. The PCR protocol
363 consisted of an initial denaturation at 95°C for 30 min, followed by 40 cycles of 95°C for
364 10 sec and 60°C for 30 sec. Relative gene expression was calculated using the $2^{-\Delta\Delta C_T}$
365 method (***Livak and Schmittgen, 2001***). The primers described previously were used
366 (***Huang et al., 2017***):

dpp primer-1: 5'-TACCACGCCATCCACTCAAC-3'

dpp primer-2: 5'-GCTCGTTACTCGATACGGCT-3'

gbb primer-1: 5'-CTGGATCATCGCACCAGAGG-3'

gbb primer-2: 5'-GTCTGGACGATCGCATGGTT-3'

rp49 (internal control) primer-1: 5'-CACCGGATTCAAGAAGTTCC-3'

rp49 (internal control) primer-2: 5'-GACAATCTCCTTGCGCTTCT-3'

Acknowledgements

We thank Eric Baehrecke, Michael Buszczak, Zheng Guo, Ed Laufer, Ruth Lehmann, Rongwen Xi, Ting Xie, Zhaohui Wang, BDGP, BDSC, DSHB, and THFC for providing antibodies, plasmids, and fly strains. This study was supported by grants 32270841 and 32070871 from the National Natural Science Foundation of China (NSFC) to Shaowei Zhao.

Author contributions

S.Z. conceived and supervised this study. Y.Z., Y.W., J.S., L.Y., Z.W., D.S., Y.D.Z., and S.Z. performed the experiments. S.Z. wrote the manuscript and all authors commented on it.

Declaration of interests

The authors declare no competing interests.

385 **References**

386 Blanpain, C., and Fuchs, E. (2006). Epidermal stem cells of the skin. Annu Rev Cell Dev
387 Biol *22*, 339-373.
388 Bopp, D., Horabin, J.I., Lersch, R.A., Cline, T.W., and Schedl, P. (1993). Expression of
389 the Sex-lethal gene is controlled at multiple levels during Drosophila oogenesis.
390 Development *118*, 797-812.
391 Chen, D., and McKearin, D. (2003a). Dpp signaling silences bam transcription directly to
392 establish asymmetric divisions of germline stem cells. Curr Biol *13*, 1786-1791.
393 Chen, D., and McKearin, D. (2005). Gene circuitry controlling a stem cell niche. Curr Biol
394 *15*, 179-184.
395 Chen, D., and McKearin, D.M. (2003b). A discrete transcriptional silencer in the bam
396 gene determines asymmetric division of the Drosophila germline stem cell. Development
397 *130*, 1159-1170.
398 Chen, D., Wu, C., Zhao, S., Geng, Q., Gao, Y., Li, X., Zhang, Y., and Wang, Z. (2014).
399 Three RNA binding proteins form a complex to promote differentiation of germline stem
400 cell lineage in Drosophila. PLoS Genet *10*, e1004797.
401 Fuller, M.T., and Spradling, A.C. (2007). Male and female Drosophila germline stem
402 cells: two versions of immortality. Science *316*, 402-404.
403 Gehart, H., and Clevers, H. (2019). Tales from the crypt: new insights into intestinal stem
404 cells. Nat Rev Gastroenterol Hepatol *16*, 19-34.
405 Germani, F., Bergantinos, C., and Johnston, L.A. (2018). Mosaic Analysis in Drosophila.
406 Genetics *208*, 473-490.
407 Huang, J., Reilein, A., and Kalderon, D. (2017). Yorkie and Hedgehog independently
408 restrict BMP production in escort cells to permit germline differentiation in the Drosophila
409 ovary. Development *144*, 2584-2594.
410 Jin, Z., Kirilly, D., Weng, C., Kawase, E., Song, X., Smith, S., Schwartz, J., and Xie, T.
411 (2008). Differentiation-defective stem cells outcompete normal stem cells for niche
412 occupancy in the Drosophila ovary. Cell Stem Cell *2*, 39-49.
413 Jogi, A., Vaapil, M., Johansson, M., and Pahlman, S. (2012). Cancer cell differentiation
414 heterogeneity and aggressive behavior in solid tumors. Ups J Med Sci *117*, 217-224.
415 Kai, T., and Spradling, A. (2003). An empty Drosophila stem cell niche reactivates the
416 proliferation of ectopic cells. Proc Natl Acad Sci U S A *100*, 4633-4638.
417 Kai, T., Williams, D., and Spradling, A.C. (2005). The expression profile of purified
418 Drosophila germline stem cells. Dev Biol *283*, 486-502.
419 Lavoie, C.A., Ohlstein, B., and McKearin, D.M. (1999). Localization and function of Bam
420 protein require the benign gonial cell neoplasm gene product. Dev Biol *212*, 405-413.
421 Li, X., Yang, F., Chen, H., Deng, B., Li, X., and Xi, R. (2016). Control of germline stem
422 cell differentiation by Polycomb and Trithorax group genes in the niche
423 microenvironment. Development *143*, 3449-3458.
424 Li, Y., Minor, N.T., Park, J.K., McKearin, D.M., and Maines, J.Z. (2009). Bam and Bgcn
425 antagonize Nanos-dependent germ-line stem cell maintenance. Proc Natl Acad Sci U S
426 A *106*, 9304-9309.
427 Lin, H. (1997). The tao of stem cells in the germline. Annu Rev Genet *31*, 455-491.
428 Lin, H., Yue, L., and Spradling, A.C. (1994). The Drosophila fusome, a germline-specific
429 organelle, contains membrane skeletal proteins and functions in cyst formation.
430 Development *120*, 947-956.
431 Livak, K.J., and Schmittgen, T.D. (2001). Analysis of relative gene expression data using
432 real-time quantitative PCR and the 2(-Delta Delta C(T)) Method. Methods *25*, 402-408.
433 Lytle, N.K., Barber, A.G., and Reya, T. (2018). Stem cell fate in cancer growth,
434 progression and therapy resistance. Nat Rev Cancer *18*, 669-680.

Mathieu, J., Michel-Hissier, P., Boucherit, V., and Huynh, J.R. (2022). The deubiquitinase USP8 targets ESCRT-III to promote incomplete cell division. Science *376*, 818-823.
McKearin, D., and Ohlstein, B. (1995). A role for the Drosophila bag-of-marbles protein in the differentiation of cystoblasts from germline stem cells. Development *121*, 2937-2947.
McKearin, D.M., and Spradling, A.C. (1990). bag-of-marbles: a Drosophila gene required to initiate both male and female gametogenesis. Genes Dev *4*, 2242-2251.
Niki, Y., and Mahowald, A.P. (2003). Ovarian cystocytes can repopulate the embryonic germ line and produce functional gametes. Proc Natl Acad Sci U S A *100*, 14042-14045.
Ohlstein, B., Lavoie, C.A., Vef, O., Gateff, E., and McKearin, D.M. (2000). The Drosophila cystoblast differentiation factor, benign gonial cell neoplasm, is related to DExH-box proteins and interacts genetically with bag-of-marbles. Genetics *155*, 1809-1819.
Ohlstein, B., and McKearin, D. (1997). Ectopic expression of the Drosophila Bam protein eliminates oogenic germline stem cells. Development *124*, 3651-3662.
Pastor-Pareja, J.C., and Xu, T. (2013). Dissecting social cell biology and tumors using Drosophila genetics. Annu Rev Genet *47*, 51-74.
Song, X., Wong, M.D., Kawase, E., Xi, R., Ding, B.C., McCarthy, J.J., and Xie, T. (2004). Bmp signals from niche cells directly repress transcription of a differentiation-promoting gene, bag of marbles, in germline stem cells in the Drosophila ovary. Development *131*, 1353-1364.
Sousa-Victor, P., García-Prat, L., and Muñoz-Cánoves, P. (2022). Control of satellite cell function in muscle regeneration and its disruption in ageing. Nat Rev Mol Cell Biol *23*, 204-226.
Spradling, A., Fuller, M.T., Braun, R.E., and Yoshida, S. (2011). Germline stem cells. Cold Spring Harb Perspect Biol *3*, a002642.
Van Doren, M., Williamson, A.L., and Lehmann, R. (1998). Regulation of zygotic gene expression in Drosophila primordial germ cells. Curr Biol *8*, 243-246.
Wilkinson, A.C., Igarashi, K.J., and Nakauchi, H. (2020). Haematopoietic stem cell self-renewal in vivo and ex vivo. Nat Rev Genet *21*, 541-554.
Xie, T., and Spradling, A.C. (1998). decapentaplegic is essential for the maintenance and division of germline stem cells in the Drosophila ovary. Cell *94*, 251-260.
Xie, T., and Spradling, A.C. (2000). A niche maintaining germ line stem cells in the Drosophila ovary. Science *290*, 328-330.
Zhang, Q., Li, L., Zhang, Q., Zhang, Y., Yan, L., Wang, Y., Wang, Y., and Zhao, S. (2024). Genetic circuitry controlling Drosophila female germline overgrowth. Dev Biol *515*, 160-168.
Zhang, Q., Zhang, Y., Zhang, Q., Li, L., and Zhao, S. (2023). Division promotes adult stem cells to perform active niche competition. Genetics *224*.
Zhao, S., Fortier, T.M., and Baehrecke, E.H. (2018). Autophagy Promotes Tumor-like Stem Cell Niche Occupancy. Curr Biol *28*, 3056-3064.e3053.

Figures and figure legends

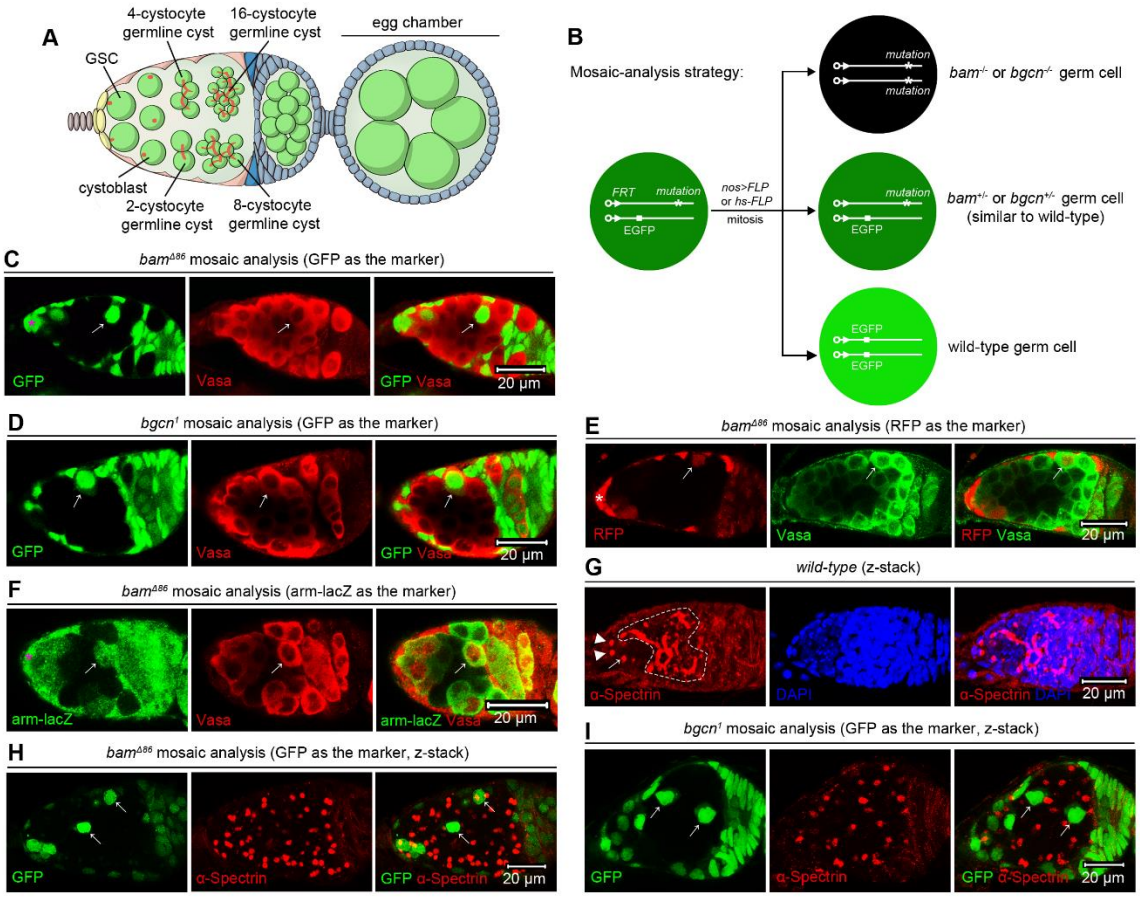

Figure 1. *bam* or *bgcn* mutant germline tumors inhibit the differentiation of neighboring wild-type GSCs. (A) Schematic cartoon for early oogenesis. The red dots and branches indicate spectrosomes and fusomes, respectively. GSC: germline stem cell. (B) Mosaic analysis strategy. The FLP recombinase triggers mitotic recombination by targeting *FRT* sequences. The *nos>FLP* method restricts FLP expression to the germline, while the *hs-FLP* method enables heatshock-inducible FLP expression. (C-F) Representative samples. The asterisks mark the niche cap cells, and the arrows indicate SGCs that have exited the niche and are surrounded by germline tumors mutant for *bam* or *bgcn*. Vasa, a germ cell marker, should label all germ cells. However, due to poor tumor permeability, staining often fails to detect tumorous germ cells in the central region (see Vasa panels in D-F). (G-I) Representative samples (z-stack projections). In (G), the

arrowheads and arrow respectively mark two GSCs and one cystoblast, all containing dot-like spectrosomes, while the dotted lines delineate cystocytes with branched fusomes. In (H) and (I), the arrows denote SGCs that also contain dot-like spectrosomes, akin to GSCs and the adjacent GSC-like tumor cells.

The online version of this article includes the following source data and figure supplement for figure 1:

Source data 1. All genotypes.

Figure supplement 1. SGCs appear in egg chambers.

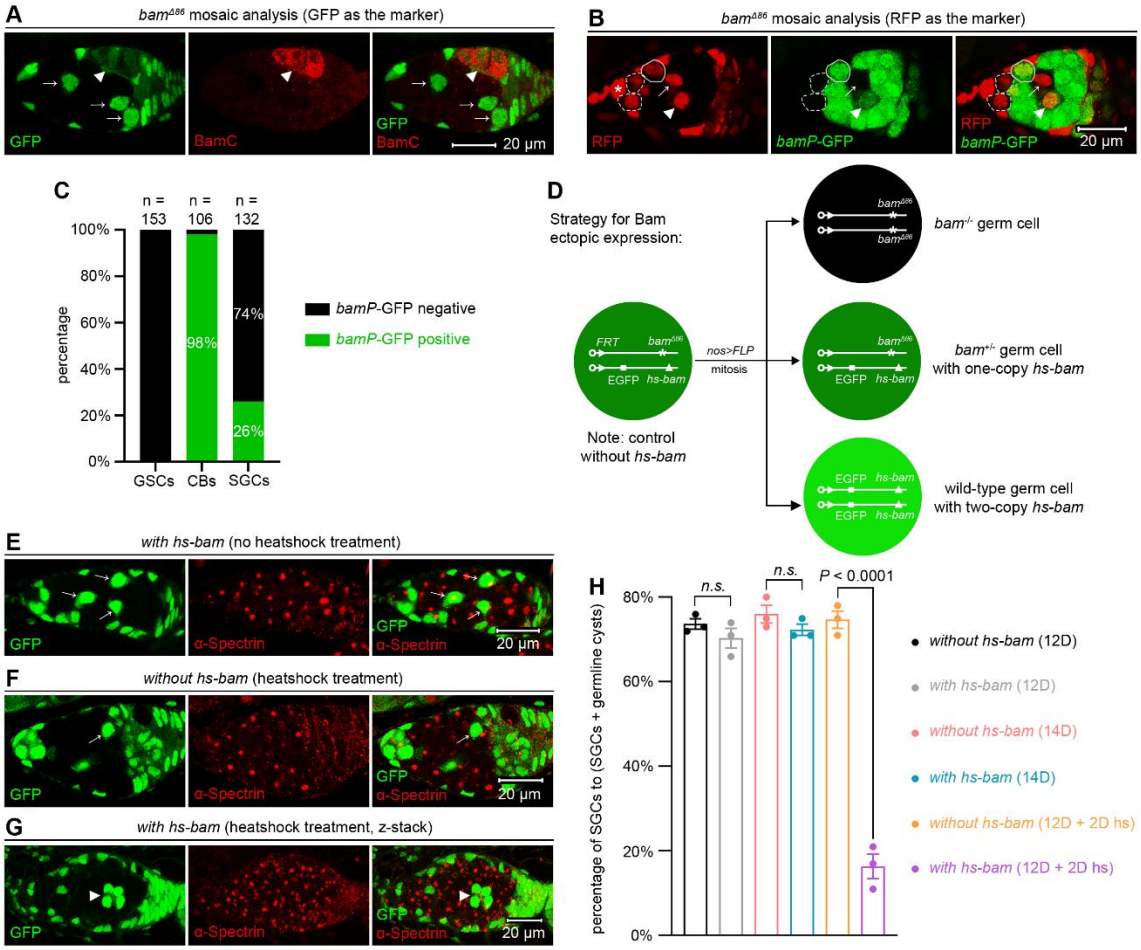

Figure 2. The inhibition of SGC differentiation depends on the lack of Bam expression. (A) Representative sample. The arrowhead marks a BamC-positive 4-cystocyte germline cyst, while the arrows indicate BamC-negative SGCs. (B) Representative sample. The asterisk denotes niche cap cells, and the dotted circles outline *bamP*-GFP-negative GSCs. The solid circle marks a *bamP*-GFP-positive cystoblast. The arrow and arrowhead point to *bamP*-GFP-negative and -positive SGCs, respectively. (C) Quantification data. 14-day-old flies were used for the analyses. CBs: cystoblasts. (D) Schematic of the experimental strategy for (E-H). In "*with hs-bam*" flies (E and G), wild-type germ cells (both $bam^{+/+}$ and $bam^{+/-}$) carry the *hs-bam* transgene, while control "*without hs-bam*" flies (F) lack this element in their wild-type germ cells. (E-G) Representative samples. The arrows mark SGCs with dot-like spectrosomes, while

509 the arrowhead indicates a 4-cystocyte germline cyst containing branched fusomes. (H)
510 Quantification data. For each experiment, three independent replicates were performed,
511 with over 100 SGCs and germline cysts quantified per replicate. Data represent mean ±
512 SEM, and statistical significance was determined by t test. *n.s.* ($P > 0.05$).
513 The online version of this article includes the following source data for figure 2:
514 **Source data 1.** All genotypes.
515 **Source data 2.** Raw quantification data.

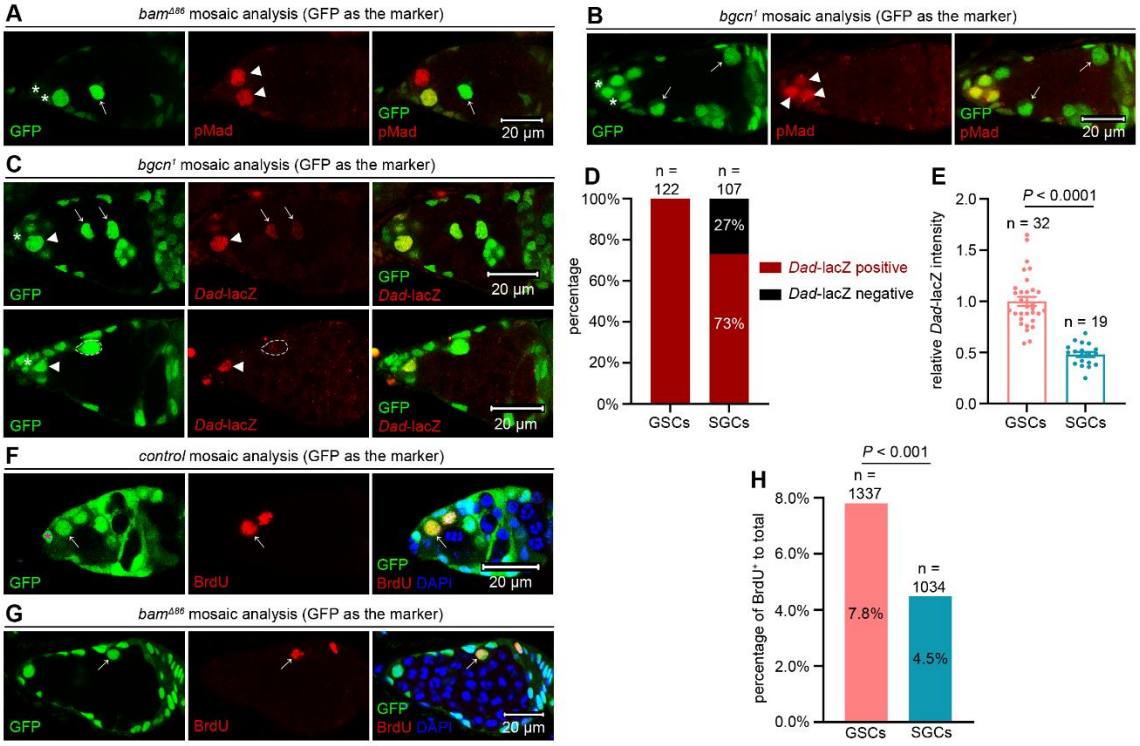

Figure 3. SGCs maintain lower BMP signaling levels than GSCs within the niche. (A and B) Representative samples. The asterisks mark niche cap cells, arrowheads indicate pMad-positive GSCs, and arrows point to pMad-negative SGCs. (C) Representative samples. The asterisks denote niche cap cells, arrowheads mark *Dad*-lacZ-positive GSCs, and arrows highlight *Dad*-lacZ-positive SGCs. The dotted cycles outline one *Dad*-lacZ-negative SGC. (D and E) Quantification data. 14-day-old flies were used for the analyses. In (E), data represent mean ± SEM, and statistical significance was determined by t test. (F) Representative sample. The asterisk marks the niche cap cell, while the arrows indicate a $BrdU^+$ GSC within the niche. (G) Representative sample. The arrow indicates a $BrdU^+$ SGC surrounded by germline tumors. (H) Quantification data. 14-day-old flies were used for the analyses. Statistical significance was determined by chi-squared test.

The online version of this article includes the following source data for figure 3:

Source data 1. All genotypes.

531 **Source data 2.** Raw quantification data.

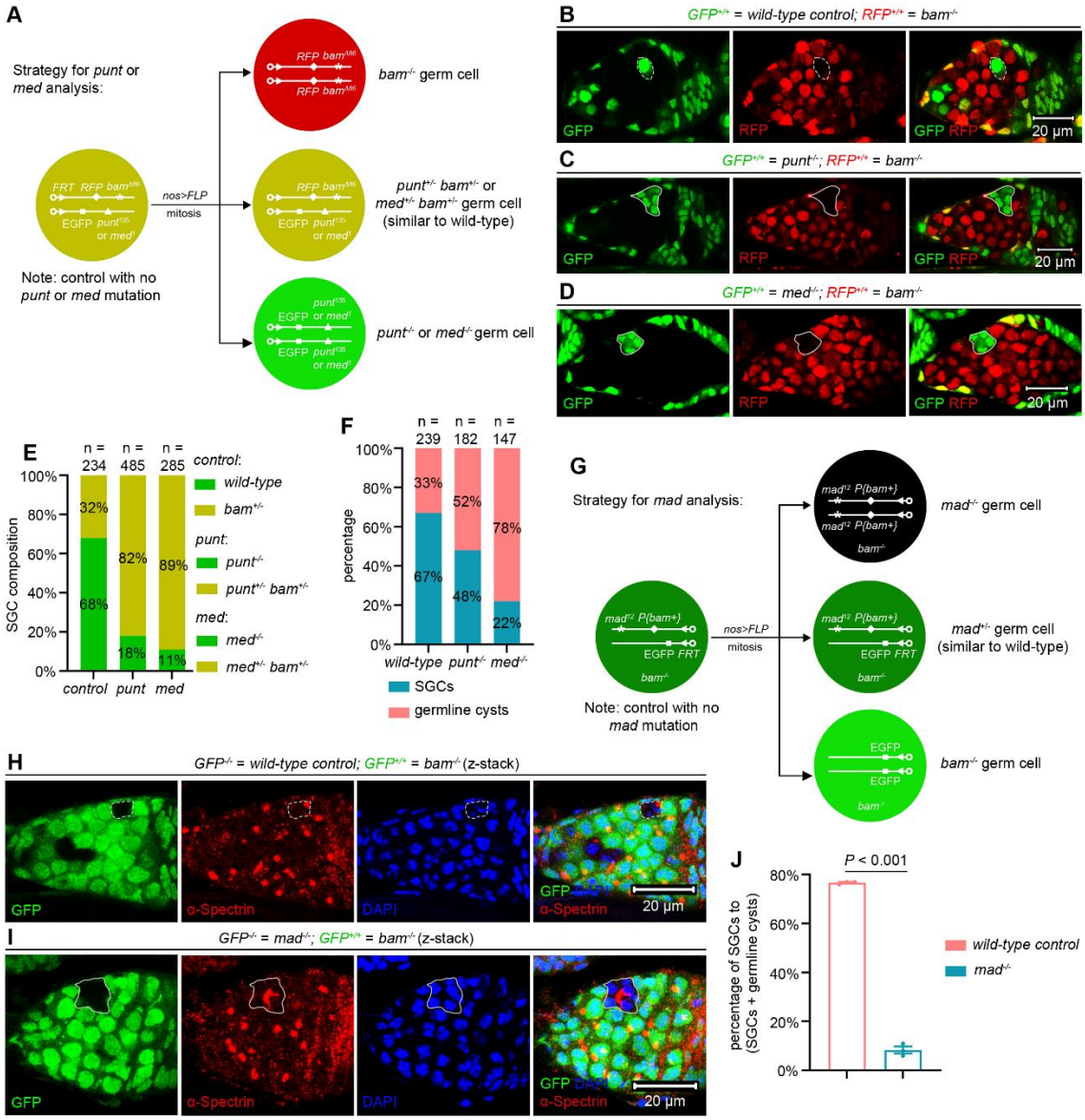

Figure 4. BMP signaling inhibits SGC differentiation. (A) Schematic of the experimental strategy for (B-F). Genotypes were unambiguously distinguished using a triple-color system (red, yellow, and green). (B-D) Representative samples. The dotted cycles mark an SGC, while the solid lines outline germline cysts containing differentiating cystocytes. (E and F) Quantification data. 14-day-old flies were used for the analyses. (G) Schematic of the experimental strategy for (H-J). (H and I) Representative samples. The dotted lines mark an SGC, while the solid lines outline a germline cyst containing differentiating cystocytes. (J) Quantification data. 14-day-old

flies were used for the analyses. For each experiment, three independent replicates were performed, with over 100 SGCs and germline cysts quantified per replicate. Data represent mean ± SEM, and statistical significance was determined by t test.

The online version of this article includes the following source data for figure 4:

Source data 1. All genotypes.

Source data 2. Raw quantification data.

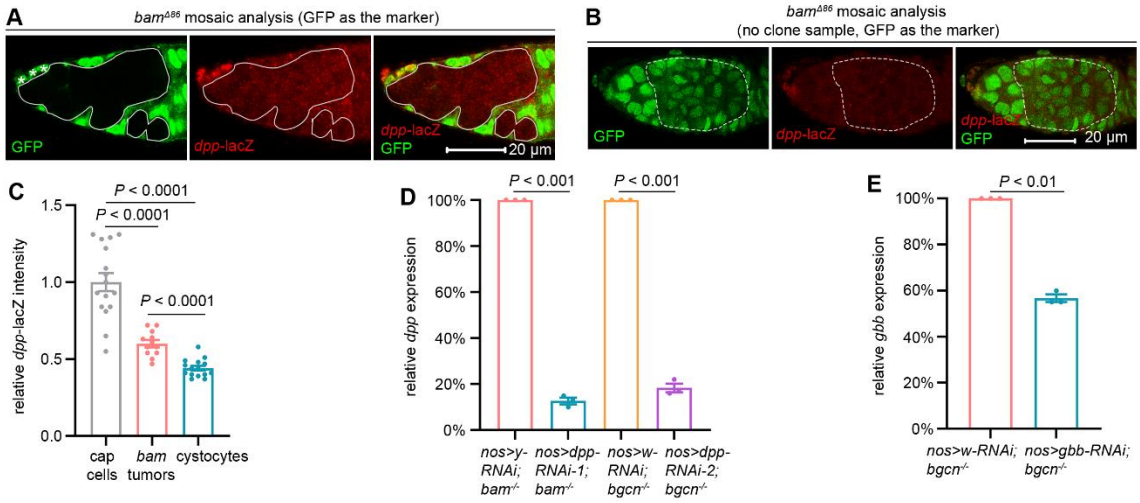

Figure 5. Germline tumors secret the BMP ligands. (A and B) Representative samples. In (A), the asterisks denote *dpp*-lacZ-high niche cap cells, and solid lines outline GFP-negative *bam* mutant germline tumor cells. In (B), the dotted lines highlight GFP-positive wild-type cystocytes. (C) Quantification data. 14-day-old flies were used for the analyses. (D and E) Quantification data for RT-qPCR assays. 14-day-old flies were used for the analyses. For each experiment, three independent replicates were performed. Statistical significance in (C) was determined by one-way ANOVA and in (D and E) by t test.

The online version of this article includes the following source data for figure 5:

Source data 1. All genotypes.

Source data 2. Raw quantification data.

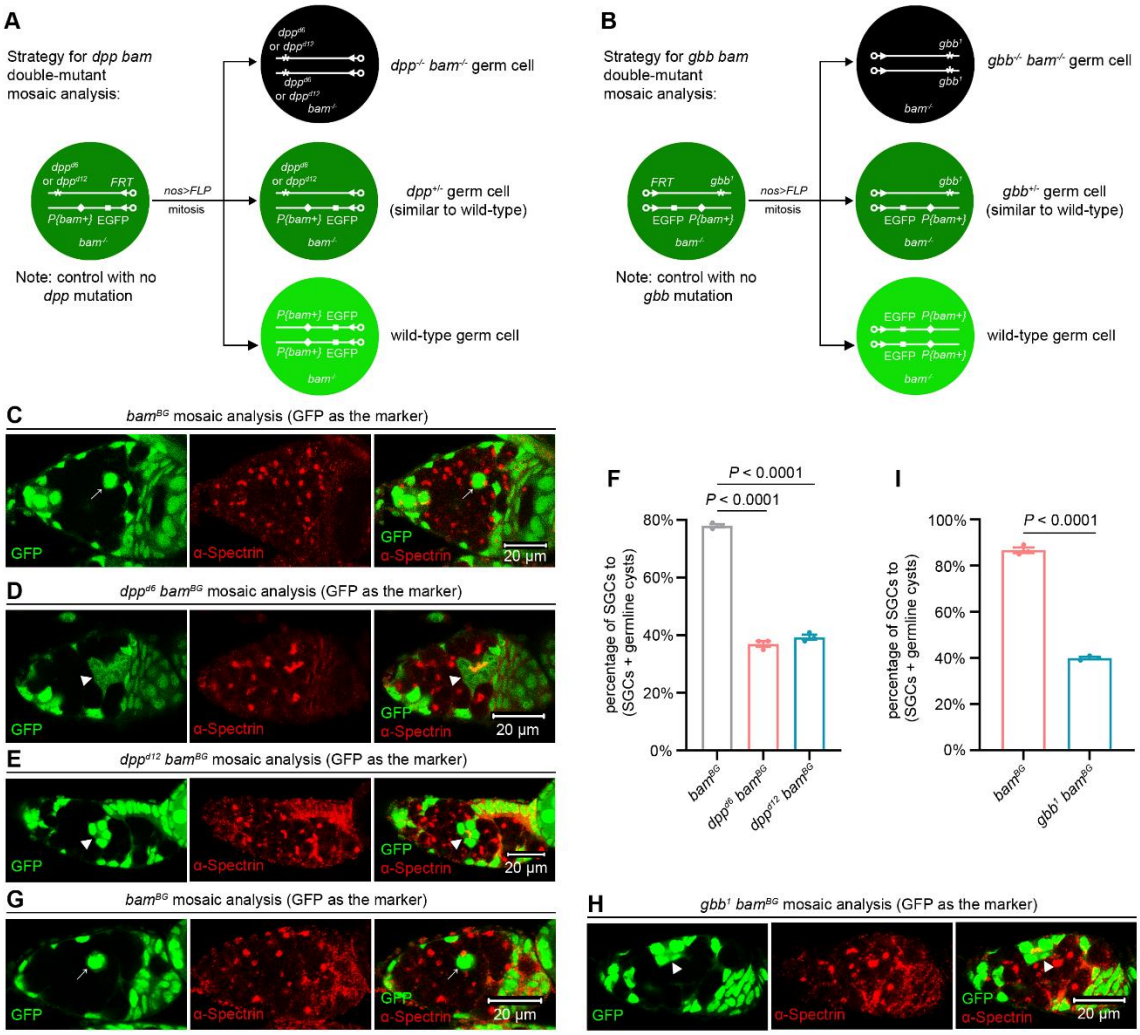

Figure 6. Dpp and Gbb secreted by germline tumors are required to inhibit SGC differentiation. (A) Schematic of the experimental strategy for (C-F). (B) Schematic of the experimental strategy for (G-I). (C-E, G, and H) Representative samples. The arrows mark SGCs containing dot-like spectrosomes, while the arrowheads denote germline cysts with differentiating cystocytes that possess branched fusomes. (F and I) Quantification data for the SGC phenotype. 14-day-old flies were used for the analyses. For each experiment, three independent replicates were performed, with over 100 SGCs and germline cysts quantified per replicate. Data represent mean ± SEM. Statistical significance in (F) was determined by one-way ANOVA and in (I) by t test.

569 The online version of this article includes the following source data and figure
570 supplement for figure 6:
571 **Source data 1.** All genotypes.
572 **Source data 2.** Raw quantification data.
573 **Figure supplement 1.** Monoallelic deletion of *dpp* or *gbb* does not affect GSC
574 maintenance, germ cell differentiation, and female fly fertility.
575 **Figure supplement 2.** *dpp bam* or *gbb bam* double-mutant germline tumor cells divide
576 more slowly than *bam* single-mutant ones.
577 **Figure supplement 3.** The SGC phenotype is unchanged irrespective of the number of
578 surrounding germline tumors.

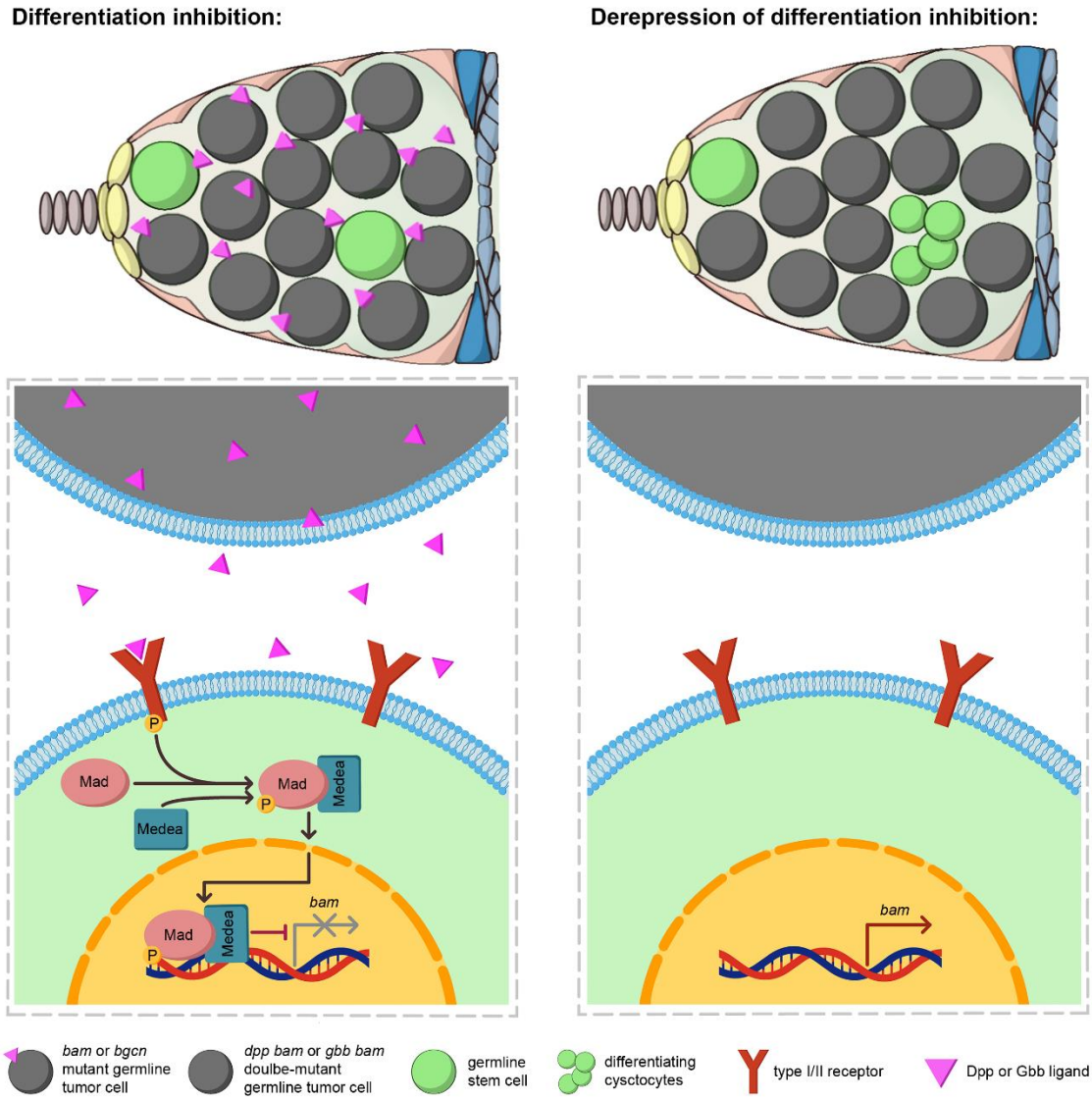

579

580 **Figure 7. A working model.** *bam* or *bgcn* mutant germline tumors secrete the BMP
581 ligands Dpp and Gbb to activate BMP signaling in out-of-niche GSCs (called SGCs in
582 this study) to inhibit their differentiation (left panel). In contrast, *dpp bam* and *gbb bam*
583 double-mutant germline tumors exhibit a significant loss of this differentiation-inhibiting
584 ability (right panel).

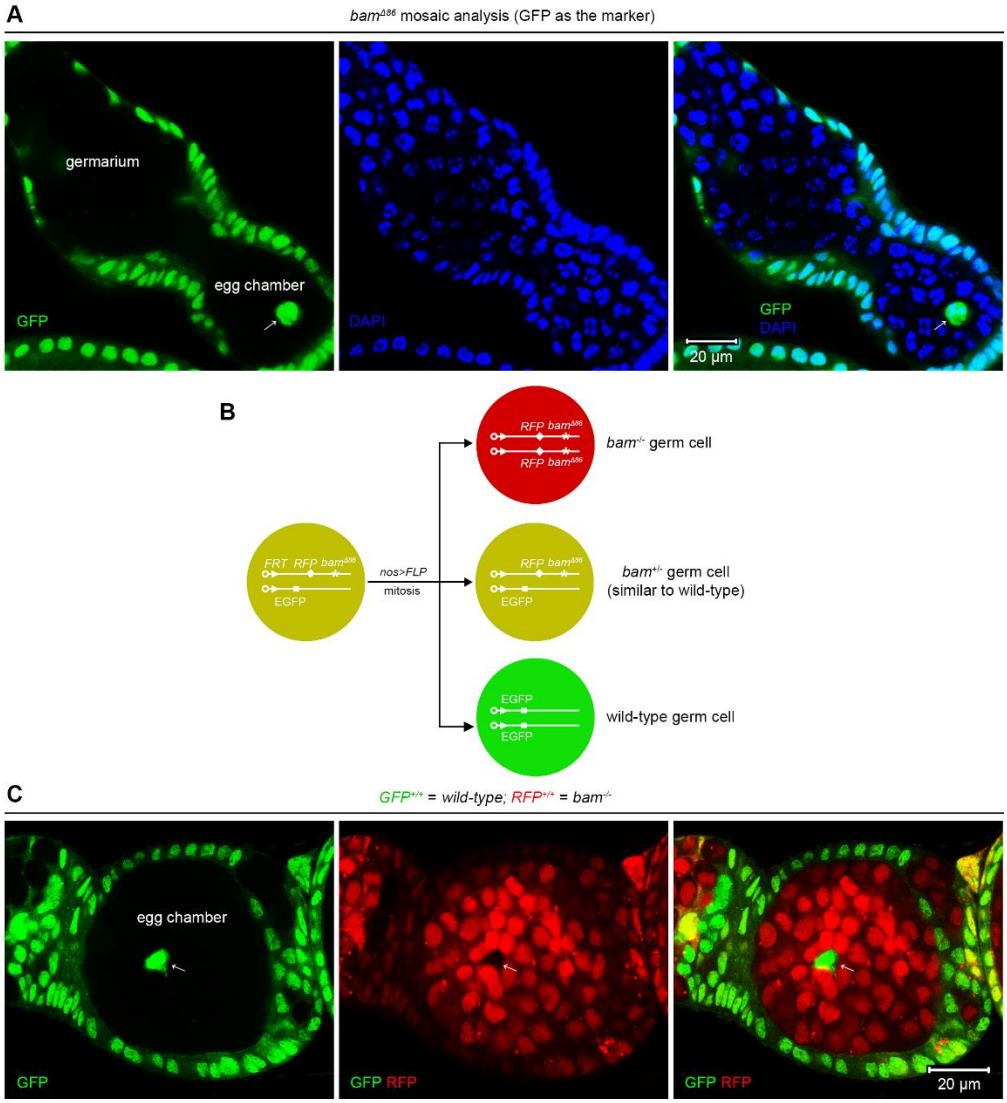

585

586 **Figure 1-figure supplement 1. SGCs appear in egg chambers.** (A, C) Representative
587 samples. The arrows indicate SGCs enclosed within egg chambers. (B) Schematic of
588 the experimental strategy for (C). See also **Source data 1**.

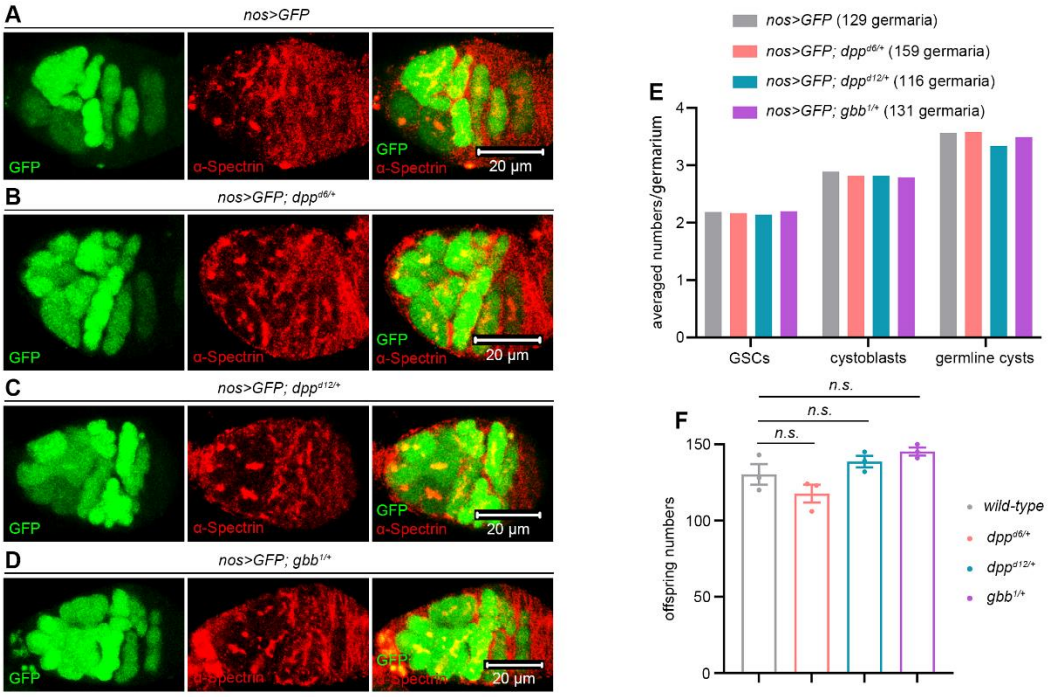

589

590 **Figure 6-figure supplement 1. Monoallelic deletion of *dpp* or *gbb* does not affect**
591 **GSC maintenance, germ cell differentiation, and female fly fertility.** (A-D)
592 Representative samples. (E) Quantification data. 14-day-old flies were used for the
593 analyses. GSCs are germ cells that are located within the niche and contain dot-like
594 spectrosomes. Cystoblasts are germ cells that have exited the niche, remain in contact
595 with GSCs, and maintain dot-like spectrosomes. Cystocytes in germline cysts are germ
596 cells that are characterized by branched fusomes. (F) Fertility test. 3-day-old flies were
597 used for the analyses. For each genotype, three independent replicates were performed.
598 Data represent mean ± SEM, and statistical significance was determined by one-way
599 ANOVA. *n.s.* ($P > 0.05$). See also **Source data 1 and 2**.

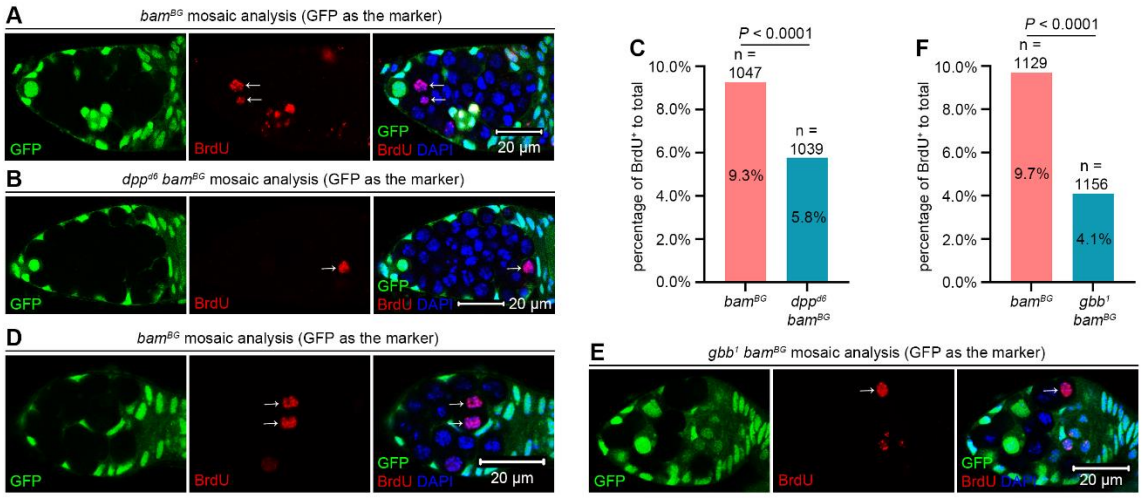

Figure 6-figure supplement 2. *dpp bam* or *gbb bam* double-mutant germline tumor cells divide more slowly than *bam* single-mutant ones. (A, B, D, and E) Representative samples. The arrows indicate BrdU$^+$ germline tumor cells mutant for *bam*, *dpp bam*, or *gbb bam*. (C and F) Quantification data. 14-day-old flies were used for the analyses. Statistical significance was determined by chi-squared test. See also **Source data 1 and 2**.

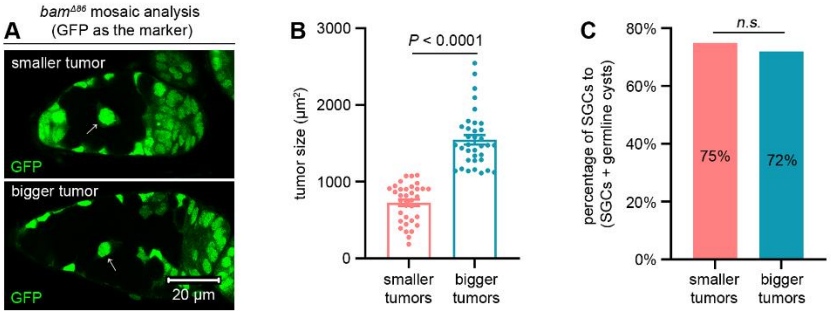

Figure 6-figure supplement 3. The SGC phenotype is unchanged irrespective of the number of surrounding germline tumors. (A) Representative samples. The arrows denote SGCs. Both images are of the same magnification. (B) Quantification data for tumor size. Data represent mean ± SEM. (C) Quantification data for the SGC phenotype. In (B and C), 14-day-old flies were used for the analyses. Statistical significance in (B) was determined by t test and in (C) by chi-squared test. *n.s.* ($P > 0.05$). See also **Source data 1 and 2**.